Diastereomeric 1,4,7,10-Tetrakis((*S*)-2-hydroxypropyl)-1,4,7,10-tetraazacyclododecane and Its Alkali Metal Complex Ions. A Nuclear Magnetic Resonance, Potentiometric Titration, and Molecular Orbital Study

Ramesh S. Dhillon,† Samer E. Madbak,† Frank G. Ciccone,† Mark A. Buntine,† Stephen F. Lincoln,*,† and Kevin P. Wainwright‡

Contribution from the Departments of Chemistry, University of Adelaide, Adelaide SA 5005, Australia, and The Flinders University of South Australia, GPO Box 2100, Adelaide 5001, Australia

Received January 22, 1997⊗

Abstract: ^{13}C NMR studies are consistent with 1,4,7,10-tetrakis((*S*)-2-hydroxypropyl)-1,4,7,10-tetraazacyclododecane (ΛS-thpc12) and its eight-coordinate alkali metal complex ions ($\Lambda[M(S\text{-thpc12})]^+$) existing predominantly as single distorted cubic diastereomers in methanol in accord with structures predicted through molecular orbital calculations. Intramolecular exchange in ΛS-thpc12 is characterized by k(298.2 K) = 34 800 ± 1600 s^{-1}, $\Delta H^{\ddagger}$ = 53.9 ± 0.6 kJ mol^{-1}, and $\Delta S^{\ddagger}$ = 22.8 ± 2.5 J K^{-1} mol^{-1} in methanol. This process is slowed in $[M(S\text{-thpc12})]^+$, for which k(298.2 K) = 332 ± 6, 125 ± 2, and 3020 ± 30 s^{-1}, $\Delta H^{\ddagger}$ = 21.4 ± 0.2, 26.3 ± 0.5, and 46.3 ± 0.2 kJ mol^{-1}, and $\Delta S^{\ddagger}$ = −125 ± 1, −116 ± 2, and −23.1 ± 0.9 J K^{-1} mol^{-1}, respectively, when $M^+ = Li^+$, Na^+, and K^+. For intermolecular ligand exchange on $\Lambda[M(S\text{-thpc12})]^+$, decomplexation is characterized by k_d(298.2 K) = 2200 ± 10, 64.3 ± 1.6, and 11 900 ± 300 s^{-1}, $\Delta H_d^{\ddagger}$ = 35.3 ± 0.5, 62.8 ± 0.5, and 41.8 ± 0.4 kJ mol^{-1}, and $\Delta S_d^{\ddagger}$ = −62.6 ± 2.1, 0.3 ± 2.0, and −26.8 ± 1.6 J K^{-1} mol^{-1}, respectively, when $M^+ = Li^+$, Na^+, and K^+. The stability constant, K, of $[M(S\text{-thpc12})]^+$ varies as M^+ changes in the sequence Li^+ (4.0 ± 0.1), Na^+ (4.8 ± 0.1), K^+ (3.5 ± 0.1), Rb^+ (3.4 ± 0.1), Cs^+ (3.2 ± 0.1), and Ag^+ (12.8 ± 0.1), where the figures in parentheses are log(K/dm^3 mol^{-1}) determined in methanol by potentiometric titration at 298.2 K and I = 0.05 mol dm^{-3} (NEt_4ClO_4). Stability constants in acetonitrile, propylene carbonate, and dimethylformamide are also reported.

Introduction

The smaller macrobicyclic cryptands are pre-eminent examples of ligands possessing preformed cavities of low flexibility which exert size selectivity in complexing metal ions.[1] The monocyclic coronands[2] and other macrocyclic and pendant arm macrocyclic ligands tend to form cavities around the metal ion during the complexation process and because of their greater flexibility are less selective.[3−7] However, such flexibility does not preclude the formation of dominant free ligand conformations in solution as we now report in apparently the first kinetic, thermodynamic, and molecular orbital study of a pendant arm macrocyclic ligand possessing a preformed cavity. Thus, Λ-1,4,7,10-tetrakis((*S*)-2-hydroxypropyl)-1,4,7,10-tetraazacyclododecane (ΛS-thpc12) exists predominantly as a single diastereomer which ^{13}C NMR spectroscopy and molecular orbital calculations using Gaussian 94[8] show to have a distorted cubic structure incorporating a cavity delineated by the parallel square planes of four oxygens and four nitrogens. It exchanges

† University of Adelaide.

‡ The Flinders University of South Australia.

⊗ Abstract published in *Advance ACS Abstracts,* June 1, 1997.

(1) (a) Lehn, J.-M.; Sauvage, J. P. *J. Am. Chem. Soc.* **1975**, *97*, 6700−6707. (b) Lehn, J.-M. *Acc. Chem. Res.* **1978**, *11*, 49−57. (c) Lehn, J.-M. *J. Inclusion Phenom.* **1988**, *6*, 351−397.

(2) (a) Pedersen, C. J. *J. Am. Chem. Soc.* **1967**, *89*, 2495−2496. (b) Pedersen, C. J. *J. Inclusion Phenom.* **1988**, *6*, 337−350.

(3) (a) Kaden, T. A. *Top. Curr. Chem.* **1984**, *121*, 157−179. (b) Lincoln, S. F.; Brereton, I. M.; Spotswood, T. M., *J. Am. Chem. Soc*. **1986**, *108*, 8134−8138. (c) Cram, D. J. *Angew. Chem., Int. Ed. Engl.* **1986**, *25*, 1039−1057. (d) Cram, D. J. *J. Inclusion Phenom*. **1988**, *6*, 397−413. (e) Lindoy, L. F. *The Chemistry of Macrocyclic Ligand Complexes*; Cambridge University Press: Cambridge, U.K., 1989. (f) Abou-Hamdan, A.; Lincoln, S. F. *Inorg. Chem*. **1991**, *30*, 462−666. (g) Hancock, R. D. In *Perspectives in Coordination Chemistry*; Williams, A. F., Floriani, C., Merbach, A. E., Eds.; VCH: Cambridge, U.K., 1992. (f) Gokel, G. W. *Chem. Soc. Rev.* **1992**, 39−47. (h) Lucas, J. B.; Lincoln, S. F. *J. Chem. Soc., Dalton Trans*. **1994**, 423−427.

(4) Turonek, M. L.; Clarke, P.; Laurence, G. S.; Lincoln, S. F.; Pittet, P.-A.; Politis, S.; Wainwright, K. P. *Inorg. Chem*. **1993**, *32*, 2195−2198.

(5) Dhillon, R.; Stephens, A. K. W.; Whitbread, S. L.; Lincoln, S. F.; Wainwright, K. P. *J. Chem. Soc., Chem. Commun.* **1995**, 97−98.

(6) Whitbread, S. L.; Politis, S.; Stephens, A. K. W.; Lucas, J. B.; Dhillon, R.; Lincoln, S. F.; Wainwright, K. P. *J. Chem. Soc., Dalton Trans*. **1996**, 1379−1384.

(7) Stephens, A. K. W.; Dhillon, R. S.; Madbak, S. E.; Whitbread, S. L.; Lincoln, S. F. *Inorg. Chem*. **1996**, *35*, 2019−2024.

(8) Gaussian 94, Revision C.3: Frisch, M. J.; Trucks, G. W.; Schlegel, H. B.; Gill, P. M. W.; Johnson, B. G.; Robb, M. A.; Cheeseman, J. R.; Keith, T.; Petersson, G. A.; Montgomery, J. A.; Raghavachari, K.; Al-Laham, M. A.; Zakrzewski, V. G.; Ortiz, J. V.; Foresman, J. B.; Cioslowski, J.; Stefanov, B. B.; Nanayakkara, A.; Challacombe, M.; Peng, C. Y.; Ayala, P. Y.; Chen, W.; Wong, M. W.; Andres, J. L.; Replogle, E. S.; Gomperts, R.; Martin, R. L.; Fox, D. J.; Binkley, J. S.; Defrees, D. J.; Baker, J.; Stewart, J. P.; Head-Gordon, M.; Gonzalez, C.; Pople, J. A. Gaussian, Inc., Pittsburgh, PA, 1995. The use of Gaussian 94[8] was tested in computing the structure of $\Lambda[Pb(S\text{-thpc12})]^{2+}$ for comparison with the distorted cubic structure observed in the solid state.[9] The global energy-mininimized structure obtained possesses C_4 symmetry and shows an approximately square anti-prismatic orientation of the two square planes delineated by the four oxygens and the four nitrogens with Pb^{2+} centrally located between them. The bidentate pendant arms are oriented in an anticlockwise direction with the methyl groups pointing out from the structure when viewed from above the square plane delineated by the four hydroxy groups, in a diastereomeric structure similar to that observed in the solid state. All four computed Pb−O distances are 274 pm, which compares with 271, 271, 278, and 278 pm in the solid state, and all four computed Pb−N distances are 272 pm, which compares with the average Pb−N distance of 264 pm (taken from structures of complex ions of cyclen) employed in solving the solid state structure. The computed twist angle is 16.1° and the globalized minimum energy = −1302.822 962 2 hartrees. The similarity of the computed and solid state structures indicates the plausibility of using Gaussian 94 as a predictor of the conformation of free *S*-thpc12 and the structures of its alkali metal complex ions.

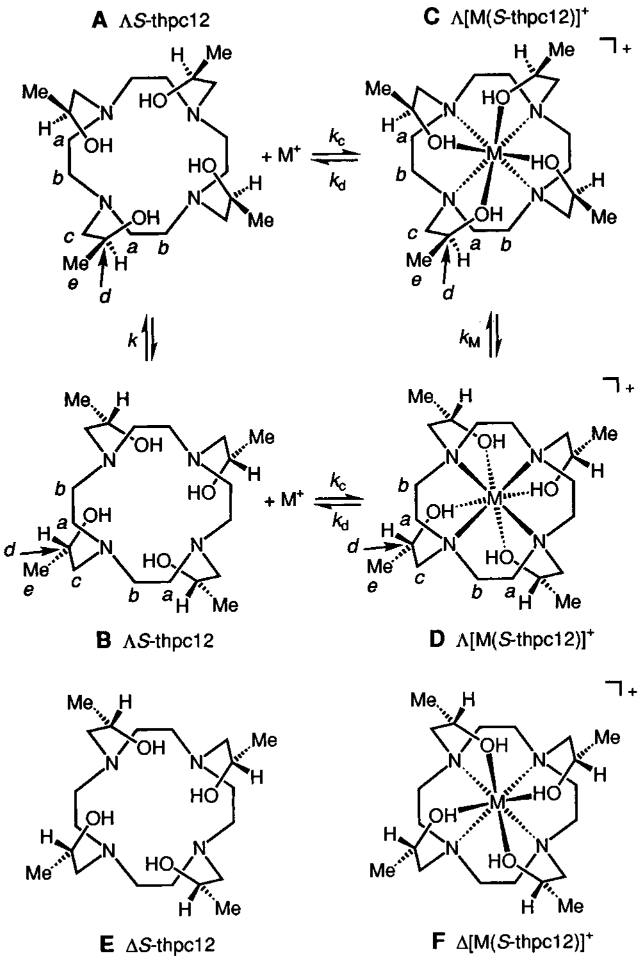

Figure 1. Equivalent representations of the Λ*S*-thpc12 diastereomer are shown as A and B, those of the Λ[M(*S*-thpc12)]$^+$ diastereomer as C and D, and the Λ*S*-thpc12 and Λ[M(*S*-thpc12)]$^+$ diastereomers as E and F, respectively. The Δ and Λ assignments are those where the four pendant arms show a clockwise and anticlockwise rotation, respectively, when viewed down the C_4 axis from the plane of the four hydroxy groups. The rotation of the plane delineated by the hydroxy groups away from eclipsing the four nitrogen plane is exaggerated to aid viewing of individual atoms. The equilibrium symbols indicate the intra- and intermolecular exchange paths.

between equivalent diastereomeric forms (Figure 1A,B) with lifetimes of 30 μs and forms alkali metal complex ions, Λ[M(*S*-thpc12)]$^+$ (Figure 1C,D), which also exist predominantly as single diastereomers with structures similar to that of Λ*S*-thpc12 with M$^+$ inside the ligand cavity which adjusts to accommodate M$^+$ size variation. The Λ[M(*S*-thpc12)]$^+$ also exchange between equivalent diastereomeric forms, but the alternative diastereomers, Δ*S*-thpc12 and Δ[M(*S*-thpc12)]$^+$ (Figure 1E,F) which appear more sterically crowded, were not detected. Our observation of the predominance of these single diastereomers coincides with Λ[Pb(*S*-thpc12)]$^{2+}$ and Λ[Bi(*S*-thpc12)]$^{3+}$ being the only diastereomers of metal complex ions of *S*-thpc12 whose solid state stuctures have been determined.[9,10]

Other studies of octadentate ligands formed through the substitution of pendant arms onto the four nitrogens of 1,4,7,10-tetraazacyclododecane have generated interest because of the high stabilities and kinetic inertness of the trivalent lanthanide complex ions formed and their potential use as contrast agents in magnetic resonance imaging[11] and as nucleases.[12] The chirality induced through eight-coordination of the ligand in these and related alkali and divalent metal ion systems has also been studied.[5−7,13,14] However, our study appears unique in detecting a single free ligand diastereomer in solution and exchange of it and its alkali metal complex ions between equivalent diastereomeric forms as shown in Figure 1.

Experimental Section

The preparation of Λ*S*-thpc12 was the same as that in the literature[9] except that (*S*)-1,2-epoxypropane (Aldrich) was used to obtain the (*S*,*S*,*S*,*S*) form exclusively. The sources of the alkali metal, silver, and tetraethylammonium perchlorates used in the titration studies were as previously described.[7] However, the K$^+$, Rb$^+$, and Cs$^+$ perchlorates were insufficiently soluble to achieve the higher concentrations required for ^{13}C NMR studies, and accordingly, the more soluble KCF_3SO_3 and its Rb$^+$ and Cs$^+$ analogues were prepared by reacting the stoichiometric amounts of K_2CO_3 (BDH), RbOH and CsOH (50% solution, Aldrich), and CF_3SO_3H (Fluka) in water and twice recrystallizing the product from water. All salts were vacuum-dried at 353−363 K for 48 h and were stored over P_2O_5 under vacuum. (***CAUTION:*** *Anhydrous perchlorate salts are oxidants and should be handled with care.*)

Acetonitrile, methanol, propylene carbonate, and dimethylformamide were purified and dried by literature methods.[15] Acetonitrile and methanol were stored over Linde 3 Å molecular sieves and the other solvents over 4 Å molecular sieves under nitrogen. The water content of these solvents was below the Karl-Fischer detection level of ∼50 ppm. Methanol-^{12}C-d_4 (99.95 atom % ^{12}C and 99.5% ^{2}H) and chloroform-*d* (99.8% ^{2}H) from Aldrich was used as received. Solutions of *S*-thpc12 and anhydrous metal perchlorates or triflates were prepared under dry nitrogen in a glovebox. For ^{13}C NMR studies, methanol-^{12}C-d_4 and chloroform-*d* solutions of *S*-thpc12 alone or with the appropriate alkali metal salt were transferred to tightly stoppered 5-mm NMR tubes. For ^{7}Li and ^{23}Na NMR studies, methanol solutions were degassed and sealed under vacuum in 5-mm NMR tubes that were coaxially mounted in 10-mm NMR tubes containing either D_2O or acetone-d_6 that provided the deuterium lock signal. The stabilities of Λ[M(*S*-thpc12)]$^+$ were such that the [ΛM(*S*-thpc12)$^+$] and free [M$^+$] and [Λ*S*-thpc12] in the solutions used in the NMR studies were close to those arising from the stoichiometric complexation. Thus, for the weakest complex, Λ[Li(*S*-thpc12)]$^+$, a solution 0.1 mol dm^{-3} in total [Li$^+$] and [Λ*S*-thpc12] will be <6% dissociated at 298.2 K. However, in the slow exchange regime at <250 K, no free Λ*S*-thpc12 was detected, consistent with an increase in stability occurring with a decrease in temperature. In studies of intermolecular M$^+$ and Λ*S*-thpc12 exchange on Λ[M(*S*-thpc12)]$^+$, concentrations were determined directly from integration under slow exchange conditions.

^{7}Li, ^{13}C (broad-band ^{1}H-decoupled), and ^{23}Na NMR spectra were run at 116.59, 75.47, and 79.39 MHz, respectively, on a Bruker CXP-300 spectrometer. In the ^{7}Li experiments, 1000−6000 transients were accumulated in a 8192 data point base over a 1000-Hz spectral width; in the ^{13}C experiments, 6000 transients were accumulated in a 8192 data point base over a 3000-Hz spectral width; and in the ^{23}Na experiments, 1000−6000 transients were accumulated in a 2048 data point base over a 8000-Hz spectral width for each solution prior to Fourier transformation. Solution temperature was controlled to within ±0.3 K using a Bruker B-VT 1000 temperature controller. The Fourier transformed spectra were subjected to complete line-shape analysis[16] on a VAX 11-780 computer to obtain rate data. The temperature-dependent ^{7}Li, ^{13}C, and ^{23}Na line widths and chemical shifts employed

(9) Hancock, R. D.; Shaikjee, M. S.; Dobson, S. M.; Boeyens, J. C. A. *Inorg. Chim. Acta* **1988**, *154*, 229−238.

(10) Luckay, R.; Reibenspies, J. H.; Hancock, R. D. *J. Chem. Soc., Chem. Commun.* **1995**, 2365−2366.

(11) (a) Desreux, J. F. *Inorg. Chem.* **1980**, *19*, 1319−1324. (b) Brittain, H. G.; Desreux, J. F. *Inorg. Chem.* **1984**, *23*, 4459−4466. (c) Loncin, M. F.; Desreux, J. F.; Merciny, E. *Inorg. Chem.* **1986**, *25*, 2646−2648. (d) Desreux, J. F.; Barthlemy, P. P. *Nucl. Med. Biol.* **1988**, *15*, 9−16. (e) Aime, S.; Botta, M.; Ermondi, G. *Inorg. Chem.* **1992**, *31*, 4291−4299.

(12) (a) Morrow, J. R.; Chin, K. O. A. *Inorg. Chem.* **1993**, *32*, 3357−3361. (b) Chin, K. O. A.; Morrow, J. R.; Lake, C. H.; Churchill, M. R. *Inorg. Chem.* **1994**, *33*, 656−664. (c) Morrow, J. R.; Aures, K.; Epstein, D. *J. Chem. Soc., Chem. Commun.* **1995**, 2431−2432.

(13) Pittet, P.-A.; Laurence; G. S.; Lincoln, S. F.; Turonek, M. L.; Wainwright, K. P. *J. Chem. Soc., Chem. Commun.* **1991**, 1205.

(14) Stephens, A. K. W.; Dhillon, R.; Lincoln, S. F.; Wainwright, K. P. *Inorg. Chim. Acta* **1995**, *236*, 185−188.

(15) Perrin, D. D.; Armarego, W. L. F.; Perrin, D. R. *Purification of Laboratory Chemicals*, 2nd ed.; Pergamon: Oxford, U.K., 1980.

(16) Lincoln, S. F. *Prog. React. Kinet.* **1977**, *9*, 1−91.

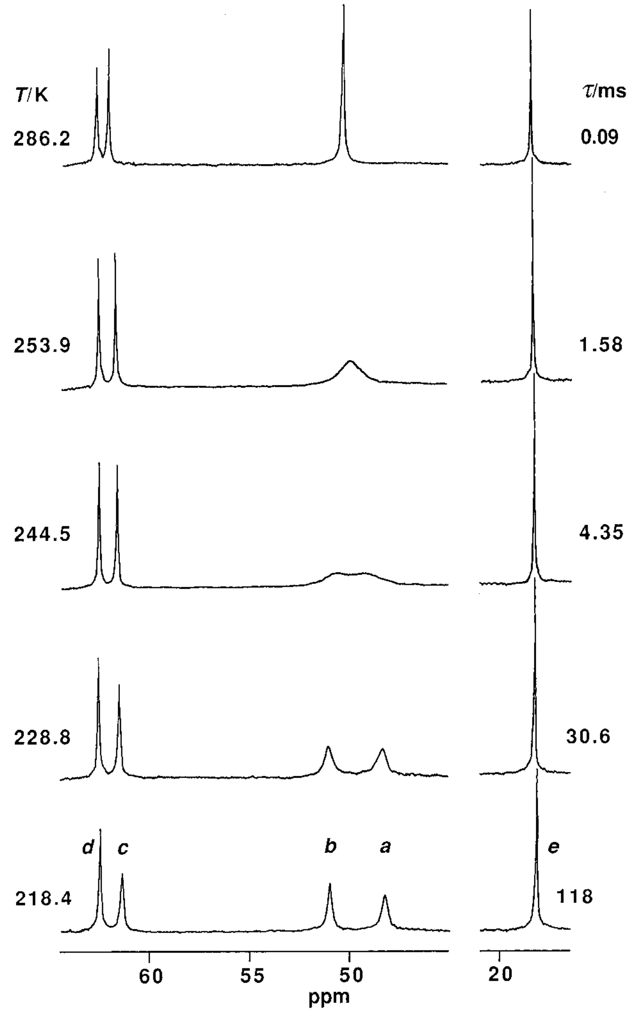

Figure 2. Temperature variation of the broad-band ^{1}H-decoupled ^{13}C NMR spectrum (75.47 MHz) of 0.10 mol dm^{-3} Λ*S*-thpc12 in methanol-^{12}C-d_4. Experimental temperatures and mean site lifetimes appear at the left and right of the figure, respectively.

in the complete line-shape analysis were obtained by extrapolation from low temperatures where no exchange-induced modification occurred. Molecular orbital calculations were carried out through Gaussian 94 using the LanL2DZ basis set[8] on a Silicon Graphics Power Challenge and a Silicon Graphics Indigo^2 work station. These calculations incorporated all electrons for H, C, N, and O, and the valence electrons for Li^+, Na^+, and K^+, together with their effective core potentials.[17] Stability constants, *K*, were determined by triplicated potentiometric titrations using a literature method.[18]

Results and Discussion

Exchange in Λ*S*-thpc12. The broad-band ^{1}H-decoupled ^{13}C NMR spectrum of Λ*S*-thpc12 in methanol-^{12}C-d_4 shows a temperature variation consistent with the occurrence of intramolecular exchange between two equivalent molecular configurations (Figure 2). At 286.2 K, the pendant arm $-C$H(CH$_3$)OH, >NCH$_2$−, and −CH(CH$_3$)OH resonances and the macrocyclic ring −CH$_2$− singlet resonance are observed at 62.55, 61.96, 18.29, and 50.22 ppm, respectively. As the temperature decreases, the pendant arm resonances broaden slightly consistent with an increase in solution viscosity while the macrocyclic ring resonance resolves into a doublet consistent with an intramolecular exchange of the macrocyclic −*C*H$_2$− between two magnetic environments, *a* and *b*, entering the slow exchange regime. Complete line-shape analysis of the coalescence of the macrocyclic −*C*H$_2$− *a* and *b* resonances yields the mean site lifetimes, τ, and the rate parameters derived through eq 1 shown in Figure 3 and in Table 1, respectively. The −*C*H(CH$_3$)OH, >N*C*H$_2$−, and −CH(*C*H$_3$)OH resonances (*c*, *d*, and *e*, respectively) are not affected by this process.

$$k = 1/\tau = (k_B T/h)\exp(-\Delta H^{\ddagger}/RT + \Delta S^{\ddagger}/R) \qquad (1)$$

The intramolecular process proposed for the distorted cubic conformation of the Λ*S*-thpc12 diastereomer in Figure 1 is consistent with the ^{13}C NMR spectral temperature variation. It is readily understood if the square plane delineated by the four nitrogens is considered fixed. Thus, Λ*S*-thpc12 (Figure 1A) has the square plane delineated by the four hydroxy groups *above* that delineated by the four nitrogens, and two environments exist for the macrocyclic −*C*H$_2$−. Double inversion at each nitrogen produces Λ*S*-thpc12 (Figure 1B). The first inversion causes each pendant arm to move below the nitrogen

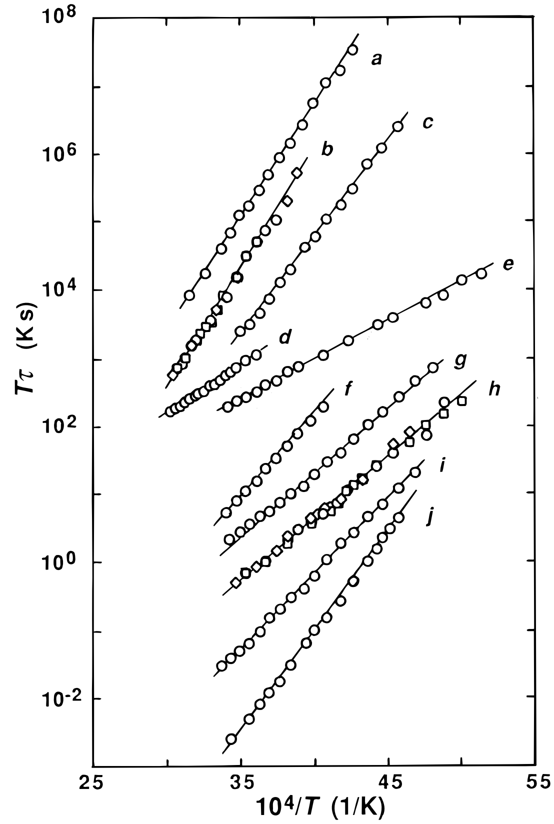

Figure 3. Temperature variations of τ for the Λ*S*-thpc12/Λ[M(*S*-thpc12)]$^+$ systems in methanol. (a) Exchange of Λ*S*-thpc12 (0.08 mol dm^{-3}) on Λ[Na(*S*-thpc12)]$^+$ (0.05 mol dm^{-3}), 8000τ_c. (b) Na^+ exchange on Λ[Na(*S*-thpc12)]$^+$, 1000τ_c. Data for the solutions in which these species were, respectively, 0.0549 and 0.0449, 0.0300 and 0.0699, and 0.0649 and 0.0350 mol dm^{-3} are represented by diamonds, squares, and circles, respectively. (c) Exchange in Λ*S*-thpc12 (0.20 mol dm^{-3}), $10^5\tau$. (d) Exchange in Λ[Na(*S*-thpc12)]$^+$ (0.10 mol dm^{-3}), 200τ. (e) Exchange in Λ[Li(*S*-thpc12)]$^+$ (0.10 mol dm^{-3}), 200τ. (f) Exchange in Λ[K(*S*-thpc12)]$^+$ (0.10 mol dm^{-3}), 40τ. (g) Exchange of Λ*S*-thpc12 (0.130 mol dm^{-3}) on Λ[Li(*S*-thpc12)]$^+$ (0.080 mol dm^{-3}), 10τ_c. (h) Li^+ exchange on Λ[Li(*S*-thpc12)]$^+$, 10τ_c. Data for the solutions in which these species were, respectively, 0.0091 and 0.0111, 0.0131 and 0.0071, and 0.0061 and 0.0141 mol dm^{-3} are represented by diamonds, squares, and circles, respectively, 2τ. (i) Exchange of *S*-thpc12 (0.050 mol dm^{-3}) on Λ[K(*S*-thpc12)]$^+$ (0.070 mol dm^{-3}), τ_c. (j) Exchange in Λ*S*-thpc12 (0.20 mol dm^{-3}) in $CDCl_3$, 0.05τ. The solid lines represent the best fits of the combined data for each group of solutions to either eq 1 or its analogue.

(17) (a) Wadt, W. R.; Hay, P. J. *J. Chem. Phys.* **1985**, *82*, 284−298. (b) Hay, P. J.; Wadt, W. R. *J. Chem. Phys.* **1985**, *82*, 299−310.
(18) (a) Cox, B. G.; Schneider, H.; Stroka, J. J. *J. Am. Chem. Soc.* **1978**, *100*, 4746−4749. (b) Cox, B. G.; Garcia-Rosas, J.; Schneider, H. *J. Am. Chem. Soc.* **1981**, *103*, 1384−1389.

Table 1. Parameters[a] for Intramolecular Exchange and Intermolecular Ligand and Metal Ion Exchange in Methanol-^{12}C-d_4

species	k (298.2 K), s^{-1}	$\Delta H^{\ddagger}$, kJ mol^{-1}	$\Delta S^{\ddagger}$, J K^{-1} mol^{-1}	k_d (298.2 K), s^{-1}	$\Delta H_d^{\ddagger}$, kJ mol^{-1}	$\Delta S_d^{\ddagger}$, J K^{-1} mol^{-1}	$10^{-5}k_c$ (298.2 K), dm^3 mol^{-1} s^{-1}
Λ*S*-thpc12	34800 ± 1600[b]	53.9 ± 0.6	22.8 ± 2.5				
Λ*S*-thpc12[c]	11300 ± 500[d]	54.3 ± 0.5	14.7 ± 2.2				
Λ[Li(*S*-thpc12)]$^+$	332 ± 6[e]	21.4 ± 0.2	−125 ± 1	2200 ± 10[f]	35.3 ± 0.5	−62.6 ± 2.1	220
				2030 ± 70[g]	34.1 ± 0.4	−67.2 ± 1.6	203
Λ[Na(*S*-thpc12)]$^+$	125 ± 2[h,i]	26.3 ± 0.5	−116 ± 2	64.3 ± 1.6[j]	62.8 ± 0.5	0.3 ± 2.0	40.6
				49.0 ± 0.7[k]	64.9 ± 0.6	5.1 ± 2.0	30.9
Λ[K(*S*-thpc12)]$^+$	3020 ± 30[l]	46.3 ± 0.2	−23.1 ± 0.9	11900 ± 300[m]	41.8 ± 0.4	−26.8 ± 1.6	375

[a] Errors represent one standard deviation. [b] Rate constant at coalescence temperature shown in brackets, k_{coal} = 240 ± 7 s^{-1} (244.5 K). [c] In $CDCl_3$. [d] k_{coal} = 209 ± 5 s^{-1} (253.8 K). [e] k_{coal} = 110 ± 1 s^{-1} (267.3 K). [f] k_{coal} = 168 ± 0.4 s^{-1} (254.9 K). [g] ^{7}Li NMR. [h] k_{coal} = 158 ± 2 s^{-1} (304.4 K). [i] Intramolecular exchange data from ref 5. [j] k_{coal} = 21.4 ± 0.5 s^{-1} (286.2 K). [k] ^{23}Na NMR. [l] k_{coal} = 475.5 ± 2.5 s^{-1} (272.5 K). [m] k_{coal} = 240 ± 5 s^{-1} (244.5 K).

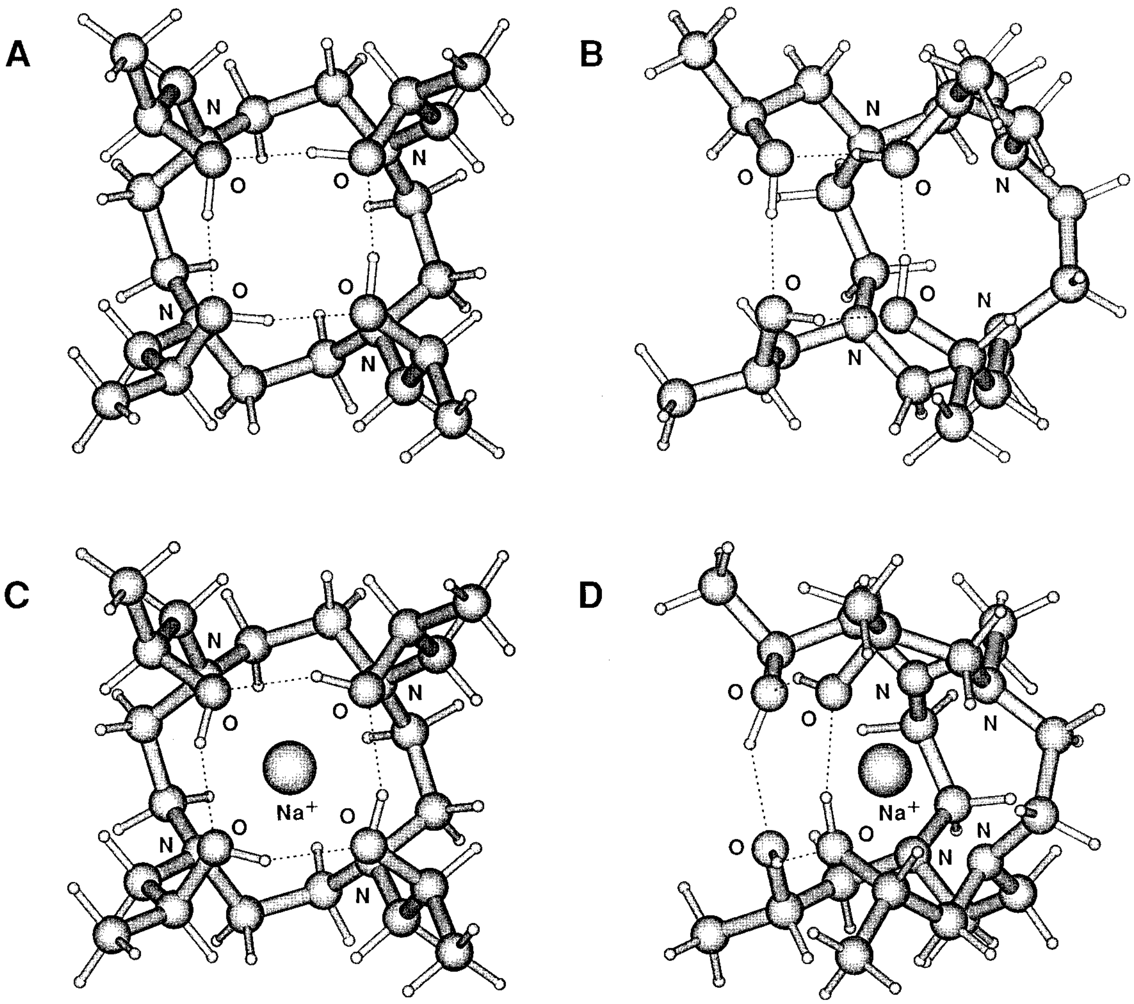

Figure 4. Global energy-minimized structures of Λ*S*-thpc12 (A and B) and Λ[Na(*S*-thpc12)]$^+$ (C and D) determined through Gaussian 94 using the LanL2DZ basis set. Hydrogen bonds are shown as broken lines. Bonds to Na^+ are not shown in C and D.

plane to produce the less stable Δ*S*-thpc12 diasteromer (equivalent to Figure 1E), and the second restores the chirality to that of the more stable Λ*S*-thpc12 diastereomer. Now the four-hydroxy plane is *below* that of the four nitrogens, and the macrocyclic $-CH_2-$ have exchanged between environments *a* and *b* while the pendant arms have exchanged between identical environments. Thus, the double inversion at each nitrogen results in exchange in a single diastereomer rather than between two diastereomers. If exchange between Δ and Λ*S*-thpc12 occurred (Figure 1, parts E and A and B), *each* diastereomer should exhibit five ^{13}C resonances in the slow exchange regime. Only one set of five resonances is observed, and it appears that only Λ*S*-thpc12 is present in detectable concentrations. Similar observations were made in chloroform-*d*, and the derived τ and rate parameters appear in Figure 3 and Table 1.

The choice of a distorted cubic structure, delineated by parallel O and N atom planes, for Λ*S*-thpc12 is consistent with the structure predicted by the molecular orbital calculations discussed below. (A distorted cubic structure is also observed in Λ[Pb(*S*-thpc12)]$^{2+}$ and Λ[Bi(*S*-thpc12)]$^{3+}$.[9,10]) In the solid state, the closely related ligand 1,4,7,10-tetrakis(2-hydroxyethyl)-1,4,7,10-tetraazacyclododecane (thec12) adopts a structure with all four pendant arms on the same side of the tetraaza plane.[19,20] It is also of interest that, in the solid state, (2*R*,5*R*,8*R*,11*R*)-2,5,8,11-tetraethyl-1,4,7,10-tetraazacyclododecane exists as a diastereomer with all four ethyl pendant arms on the same side

(19) Buøen, S.; Dale, J.; Groth, P.; Krane, J. *J. Chem. Soc., Chem. Commun.* **1982**, 1172−1174.
(20) Groth, P. *Acta Chem. Scand. A* **1983**, *37*, 75−77.
(21) Sakurai, T.; Kobayashi, K.; Tsuboyama, K.; Tsuboyama, S. *Acta Crystallogr., Sect. B* **1978**, *34*, 1144−1148.

Table 2. Parameters Derived from Molecular Orbital Calculations Using the Gaussian 94 LanL2DZ Basis Set[a]

distances, pm	ΛS-thpc12	Λ[M(S-thpc12)]$^+$		
		$M^+ = Li^+$ [b]	$M^+ = Na^+$	$M^+ = K^+$
O−O	273	O1−O2 = 270 O2−O3 = 262 O3−O4 = 269 O4−O1 = 269	275	370
N−N	317	N1−N2 = 302 N2−N3 = 303 N3−N4 = 301 N4−N1 = 304	311	320
O−N	295	O1−N1 = 289 O2−N2 = 300 O3−N3 = 278 O4−N4 = 299	293	303
M−O		Li−O1 = 269 Li−O2 = 298 Li−O3 = 225 L1−O4 = 293	254	282
M−N		Li−N1 = 238 Li−N2 = 233 Li−N3 = 228 Li−N4 = 234	254	295
M−O plane		*c*	163	106
M−N plane		*d*	128	190
H−O[e]	97	97	96	96
H−O[f]	177	H1−O4 = 180 H2−O1 = 180 H3−O2 = 171 H4−O3 = 178	190	*g*
twist angle ϕ (deg)[h]	6.1	*i*	5.3	12.5

[a] The globalized minimum energies for ΛS-thpc12 and its Li^+, Na^+, and K^+ complex ions are −1299.78, −1307.22, −1299.95, and −1327.59 hartrees, respectively, where 1 hartree = 2617.13 kJ mol^{-1}. [b] Atom numbering as in Figure 5A,B. [c] The oxygen atoms have no common plane. [d] The nitrogen atoms have no common plane. [e] The distance between H and O in hydroxy groups. [f] The distance between the H and O of adjacent hydroxy groups. [g] No hydrogen bonding. [h] Twist angle $\phi = 0°$ for a cubic structure. [i] No meaningful ϕ as C_4 symmetry is absent.

of the tetraaza plane and rotated in a clockwise direction when viewed from the pendant arm side of the tetraaza plane.[21]

Molecular Orbital Calculations. The global energy-minimized ΛS-thpc12 cubic structure calculated using Gaussian 94[8] has C_4 symmetry (Figure 4A,B) and shows near superimposition of the two parallel square planes delineated by four oxygens and four nitrogens, respectively. The hydroxy protons point toward the adjacent hydroxy oxygen and are at distances where weak hydrogen bonding exists.[22] The (S)-2-hydroxypropyl arms are oriented in an anticlockwise direction when viewed down the C_4 axis from the four oxygen plane so that the methyl groups project out from the structure and render the two carbons in each macrocyclic ethylene linkage inequivalent in broad agreement with the ΛS-thpc12 structure proposed on the basis of the ^{13}C NMR studies. Each pair of methylene carbons is equivalent to the other pairs, and a similar equivalence applies for the pendant arms. Selected interatomic distances for ΛS-thpc12 and Λ[M(S-thpc12)]$^+$ appear in Table 2.

That Figure 4A,B represents the global-minimized structure was tested by selecting four basic structures with either four, three, two adjacent, or two diagonally opposed pendant arms on the same side of the tetraaza plane as minimization starting points. A range of macrocyclic ring conformations were then superimposed on these structures to give a wide selection of starting points. In all cases, the energy-minimized structure obtained was that shown in Figure 4A,B consistent with a global energy minimum being reached. Analogous starting point structures were used to test that the Λ[M(S-thpc12)]$^+$ structures shown in Figure 4C,D and Figure 5A−D were also global-minimized structures.

The computed distorted cubic structure for Λ[Na(S-thpc12)]$^+$ (Figure 4C,D) also possesses C_4 symmetry and has chiral characteristics similar to those of ΛS-thpc12. The hydroxy protons point toward the adjacent hydroxy oxygens at distances at which weak hydrogen bonding exists.[22] The Na^+ is centrally positioned in the ligand cavity and the (S)-2-hydroxypropyl arms are oriented in an anticlockwise direction so that the methyl groups project out from the structure and render the two carbons in each macrocyclic ethylene linkage inequivalent as found in the ^{13}C NMR studies discussed below. The similarity of the Λ[Na(S-thpc12)]$^+$ and ΛS-thpc12 dimensions indicates an optimum fit of Na^+ to the ΛS-thpc12 cavity.

The computed Λ[Li(S-thpc12)]$^+$ does not possess C_4 symmetry (Figure 5A,B) as is indicated by the variation in the Li−O and Li−N distances (Table 2) consistent with Li^+ being too small for an optimum fit into the ΛS-thpc12 cavity. As a result, Λ[Li(S-thpc12)]$^+$ shows its major distance variation in the Li−O distances with one small distance and three larger ones and can be viewed as approaching a five-coordinate structure similar to that found in [Li(thec12)]$^+$ in the solid state where Li^+ is coordinated by four nitrogens and one oxygen.[19,23] However, in the [Li(thec12)]$^+$ structure, the three uncoordinated hydroxy groups form intermolecular hydrogen bonds, while in the computed Λ[Li(S-thpc12)]$^+$ structure, intramolecular hydrogen bonding between adjacent hydroxy groups occurs. Despite the absence of C_4 symmetry, Λ[Li(S-thpc12)]$^+$ retains the general Λ arrangement of the (S)-2-hydroxypropyl arms observed in ΛS-thpc12 and Λ[Na(S-thpc12)]$^+$.

In the computed structure of Λ[K(S-thpc12)]$^+$ (Figure 5C,D), the larger size of K^+ causes the O−O, O−N, K−O, and K−N distances to increase, and the hydrogen bonding between adjacent hydroxy groups is absent as a consequence. The decrease in the K−O plane distance and increase in the K−N plane distance indicates that K^+ is less well accommodated by the ΛS-thpc12 cavity than is Na^+. The three computed Λ[M(S-thpc12)]$^+$ structures possess the same macrocyclic ring conformation, which is the same as that observed in their [M(thec12)]$^+$ analogues.[19,23,24] In general terms the computed structures of ΛS-thpc12 and Λ[M(S-thpc12)]$^+$ add plausibility to the interpretation of the ^{13}C NMR data above and below in terms of single ΛS-thpc12 and Λ[M(S-thpc12)]$^+$ diastereomers.

Exchange in Λ[M(S-thpc12)]$^+$. Under slow exchange conditions at 235.9 K in methanol-^{12}C-d_4, the broad-band ^{1}H-decoupled ^{13}C NMR spectrum of Λ[Li(S-thpc12)]$^+$ (Figure 6) consists of five resonances at 62.39, 60.28, and 19.74 ppm assigned to the pendant arm −CH(CH$_3$)OH, >NCH$_2$−, and −CH(CH$_3$)OH carbons, respectively, and at 50.22 and 48.88 ppm assigned to the macrocyclic ring carbons that cannot be separately identified from these data. Five similarly assigned resonances at 62.34, 61.14, 20.08, 50.66, and 48.81 ppm are observed for Λ[Na(S-thpc12)]$^+$ and for Λ[K(S-thpc12)]$^+$ (Figure 7) at 64.13, 63.13, 20.43, 52.53, and 49.43 ppm. The two macrocyclic ring Λ[M(S-thpc12)]$^+$ resonances broaden and coalesce as the two macrocyclic ring carbons exchange between different magnetic environments. Complete line-shape analyses of these coalescences yield the τ and rate parameters in Figure 3 and and Table 1. Below 250 K, both $RbCF_3SO_3$ and $CsCF_3SO_3$ precipitated from 0.05 mol dm^{-3} solutions of these salts and S-thpc12; however, sufficient Λ[Rb(S-thpc12)]$^+$ remained in solution to observe its ^{13}C spectrum. Thus, at 210 K, separate resonances for Λ[Rb(S-thpc12)]$^+$ appeared at 66.05, 64.47, and

(22) Emsley, J. *Chem. Soc. Rev.* **1980**, *9*, 91−124.

(23) Groth, P. *Acta Chem. Scand. A* **1983**, *37*, 71−74.
(24) Groth, P. *Acta Chem. Scand. A* **1983**, *37*, 283−291.

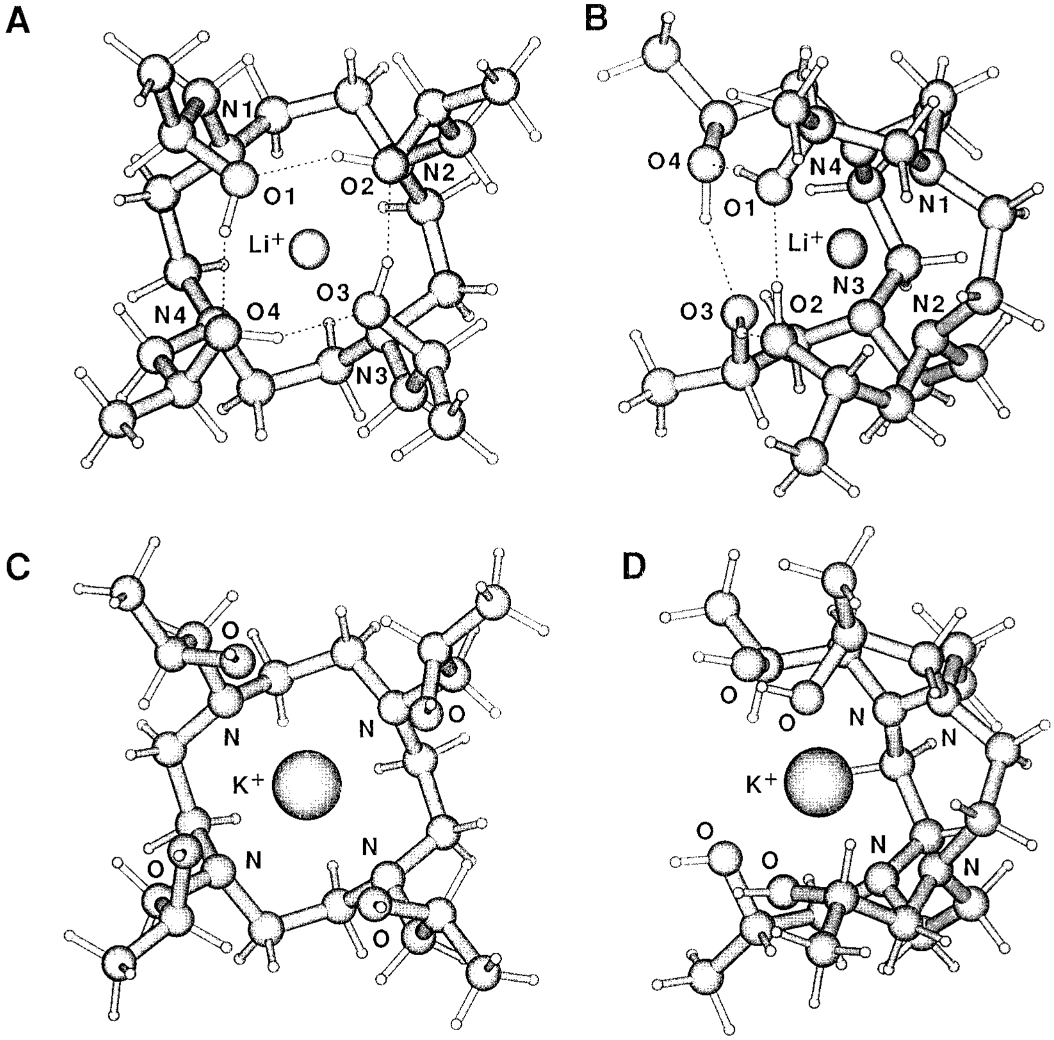

Figure 5. Global energy-minimized structures of $\Lambda[Li(S\text{-thpc12})]^+$ (A and B) and $\Lambda[K(S\text{-thpc12})]^+$ (C and D) determined through Gaussian 94 using the LanL2DZ basis set. Hydrogen bonds are shown as broken lines. Bonds to Li^+ and K^+ are not shown in A−D.

21.72 ppm assigned to the pendant arm −*C*H(CH_3)OH, >N*C*H_2−, and −CH(*C*H_3)OH carbons, respectively, and at 54.00 and 50.15 ppm assigned to the macrocyclic ring carbons, and the analogous resonances were observed at 63.53, 62.41, 19.32, 52.04, and 49.21 ppm for Λ*S*-thpc12. Only one set of five resonances is observed for each complex ion, and it is concluded that only $\Lambda[M(S\text{-thpc12})]^+$ is present at detectable concentrations.

The coalescence of the two macrocyclic ring resonances of $\Lambda[M(S\text{-thpc12})]^+$ and the absence of change in their pendant arm resonances, apart from a slight broadening attributable to solution viscosity increases at lower temperatures, is consistent with exchange between the two equivalent $\Lambda[M(S\text{-thpc12})]^+$ configurations shown in Figure 1. Thus, $\Lambda[M(S\text{-thpc12})]^+$ (Figure 1C) has the square plane delineated by the four oxygens *above* that delineated by the four nitrogens, and two environments exist for the macrocyclic −*C*H_2−. Double inversion about each nitrogen produces $\Lambda[M(S\text{-thpc12})]^+$ (Figure 1D) in which the four-oxygen plane is *below* that of the four nitrogens, and the macrocyclic −*C*H_2− exchange between environments *a* and *b* while the pendant arms exchange between identical environments. While the computed C_4 structures of $\Lambda[Na(S\text{-thpc12})]^+$ and $\Lambda[K(S\text{-thpc12})]^+$ discussed above possess the atomic equivalences required by the corresponding ^{13}C NMR spectra, the computed $\Lambda[Li(S\text{-thpc12})]^+$ structure does not. Thus, if the solution $\Lambda[Li(S\text{-thpc12})]^+$ structure is similar to the computed structure, it appears that a fluxional motion in the structure renders all (*S*)-2-hydroxypropyl arms equivalent and all macrocyclic ring ethylenic moieties equivalent at a rate in the fast exchange limit of the ^{13}C NMR time scale which is much faster than the double nitrogen inversion processes.

Double nitrogen inversion in $\Lambda[M(S\text{-thpc12})]^+$ is greatly slowed by comparison with that in Λ*S*-thpc12 (Table 1) largely because of the negative $\Delta S^{\ddagger}$ characterizing $\Lambda[M(S\text{-thpc12})]^+$, but the detailed mechanism of the inversion is unclear; however, it is possible that it involves passage of M^+ through the macrocyclic annulus. We estimate the macrocyclic hole radius as ≈127 pm from literature data[25] which is sufficient to allow Li^+ and Na^+ and possibly K^+ with some strain (four- and six-coordinate ionic radii = 59, 99, and 137, and 76, 102, and 138 ppm, respectively[26]) to pass through in a mechanism ultimately requiring the dissociation of all four M−O bonds. This mechanism is similar to the transannular oscillation mechanism proposed for 1,4,8,11-tetrakis(2-hydroxyethyl)-1,4,8,11-tetraazacyclotetradecanecadmium(II) and its Hg^{2+} and Pb^{2+} analogues.[27,28] Alternatively, M^+ may traverse the edge of the macrocyle in a process involving sequential M−N and M−O bond breaking and making to achieve the double inversion at each nitrogen. (In a preliminary study of $[Na(S\text{-thpc12})]^+$, it was suggested that variable-temperature ^{13}C NMR data could

(25) Henrick, K.; Tasker, P. A.; Lindoy, L. F. *Prog. Inorg. Chem.* **1985**, *33*, 1−58.
(26) Shannon, R. D. *Acta Crystallogr., Sect. A* **1976**, *32*, 751−767.
(27) Clarke, P.; Hounslow, A. M.; Keough, R. A.; Lincoln, S. F.; Wainwright, K. P. *Inorg. Chem.* **1990**, *29*, 1793−1797.
(28) Clarke, P.; Lincoln, S. F.; Wainwright, K. P. *Inorg. Chem.* **1991**, *30*, 134−139.

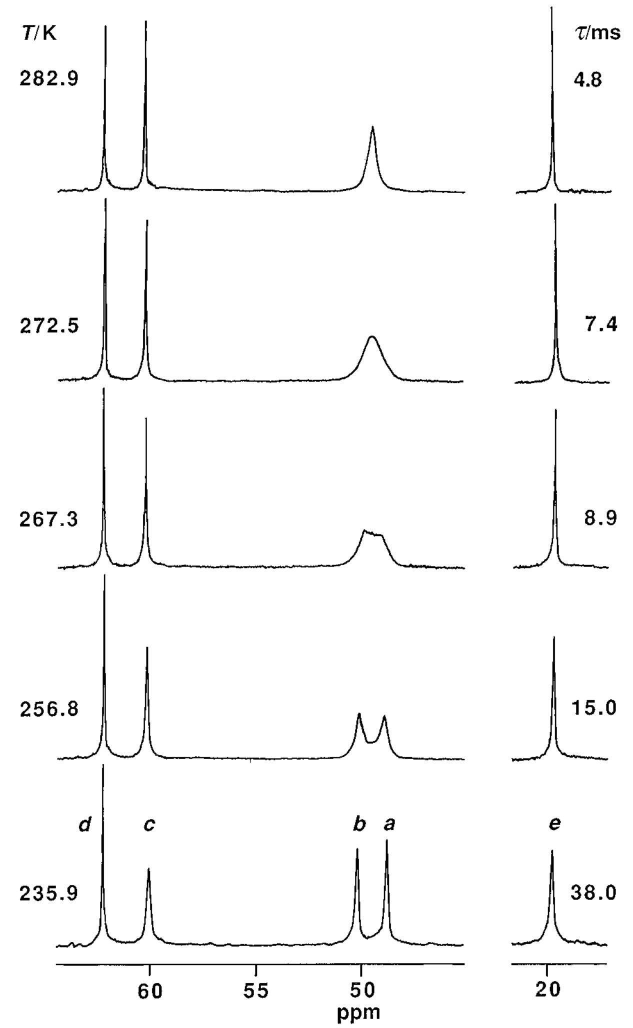

Figure 6. Temperature variation of the broad-band ^{1}H-decoupled ^{13}C NMR spectrum (75.47 MHz) of Λ[Li(*S*-thpc12)]$^{+}$ (0.10 mol dm^{-3}) in methanol-^{12}*C*-*d*$_4$. Experimental temperatures and τ values derived from complete line-shape analyses of the coalescing doublet arising from the macrocyclic ring carbons, *a* and *b*, appear to the left and right of the figure, respectively. The resonances arising from the pendant arm >N*C*H$_2$−, −*C*H(CH$_3$)OH, and −CH(*C*H$_3$)OH are labeled *c*, *d*, and *e*, respectively.

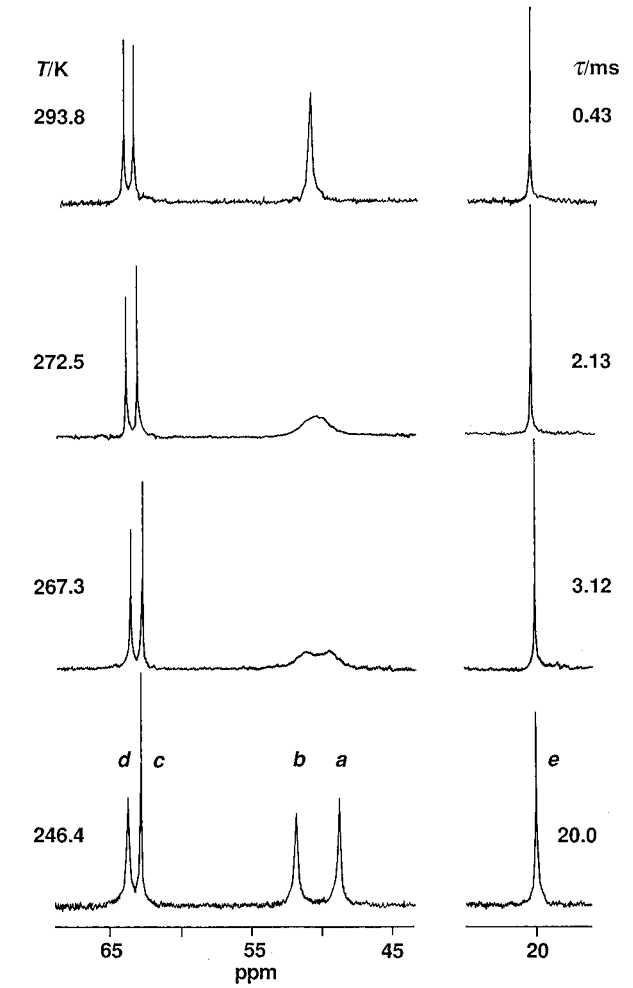

Figure 7. Temperature variation of the broad-band ^{1}H-decoupled 75.47-MHz ^{13}C NMR spectrum of Λ[K(*S*-thpc12)]$^{+}$ (0.10 mol dm^{-3}) in methanol-^{12}*C*-*d*$_4$. Experimental temperatures and τ values derived from complete line-shape analyses of the coalescing doublet arising from the macrocyclic ring carbons, *a* and *b*, appear to the left and right of the figure, respectively. The resonances arising from the pendant arm >N*C*H$_2$−, −*C*H(CH$_3$)OH, and −CH(*C*H$_3$)OH are labeled *c*, *d*, and *e*, respectively.

be interpreted in terms of exchange between Δ and Λ diastereomers which had identical ^{13}C chemical shifts.[5] Extension of this interpretation to the Li^{+} and K^{+} analogues and free *S*-thpc12 would require each of their diastereomer pairs to also possess identical ^{13}C chemical shifts which seems increasingly unlikely.)

Exchange of M^{+} and Λ*S*-thpc12 on Λ[M(*S*-thpc12)]$^{+}$. The parameters for intermolecular M^{+} exchange on Λ[M(*S*-thpc12)]$^{+}$ (Table 1) were determined from the complete line-shape analyses[16] of the temperature-dependent coalescences of the ^{7}Li and ^{23}Na resonances arising from exchange of these nuclei between the solvated M^{+} and Λ[M(*S*-thpc12)]$^{+}$ in methanol (Figure 8). The magnitude and temperature variation of the mean lifetime of Li^{+} in Λ[Li(*S*-thpc12)]$^{+}$, $\tau_c = X_c\tau_s/X_s$ (where τ_s is the mean lifetime of Li^{+} in the solvated state and X_c and X_s are the corresponding mole fractions for the Λ[Li(*S*-thpc12)]$^{+}$ solutions), are very similar for the three solutions whose compositions appear in the caption to Figure 3, and a similar situation holds for Λ[Na(*S*-thpc12)]$^{+}$. Thus, τ_c is independent of the concentration of solvated M^{+} consistent with its nonparticipation in the rate-determining step for M^{+} exchange on Λ[M(*S*-thpc12)]$^{+}$ and the predominant operation of a monomolecular mechanism for the decomplexation of M^{+} from Λ[M(*S*-thpc12)]$^{+}$ as shown in eq 2 (where the complexation rate constant is $k_c = k_d/K$, where K is the stability constant discussed below). The parameters for the decomplexation of Λ[M(*S*-thpc12)]$^{+}$ (Table 1) were derived through a simultaneous fit of the τ_c ($= 1/k_d$) data from all of the solutions studied for a particular Λ[M(*S*-thpc12)]$^{+}$ to an equation analogous to eq 1.

The intermolecular exchange of Λ*S*-thpc12 in Λ[M(*S*-thpc12)]$^{+}$ (eq 3) was followed through the coalescence of the −*C*H(CH$_3$)OH and −CH(*C*H$_3$)OH ^{13}C resonances of free and complexed Λ*S*-thpc12 (Figure 9). The mean lifetime (Figure

$$\mathrm{M}^{+} + \Lambda S\text{-thpc12} \underset{k_d}{\overset{k_c}{\rightleftharpoons}} \Lambda[\mathrm{M}(S\text{-thpc12})]^{+} \qquad (2)$$

$$\Lambda[\mathrm{M}(S\text{-thpc12})]^{+} + {}^{*}\Lambda S\text{-thpc12} \underset{k_d}{\overset{k_d}{\rightleftharpoons}} \Lambda[\mathrm{M}({}^{*}S\text{-thpc12})]^{+} + \Lambda S\text{-thpc12} \qquad (3)$$

3) of Λ*S*-thpc12 in Λ[M(*S*-thpc12)]$^{+}$, τ_c, was determined from the complete line-shape analyses of these coalescences and the activation parameters were determined from its temperature dependence for $M^{+} = Li^{+}$, Na^{+}, and K^{+} through an equation analogous to eq 1. The rate parameters for M^{+} and Λ*S*-thpc12 exchange show sufficient similarity for both processes to be considered to occur through the same monomolecular mechanism.

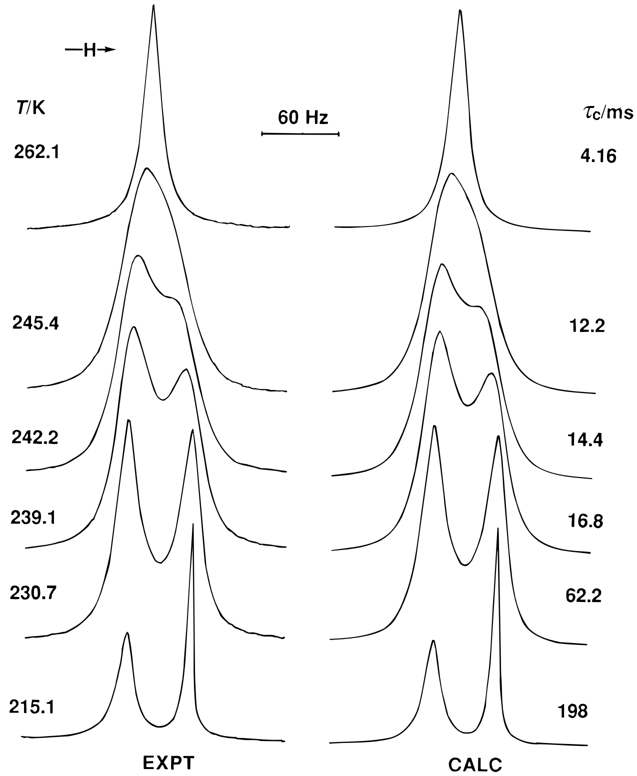

Figure 8. Typical exchange-modified 116.59-MHz ^{7}Li NMR spectra of a methanol solution of solvated Li^{+} (0.0091 mol dm^{-3}) and Λ[Li(*S*-thpc12)]$^{+}$ (0.0111 mol dm^{-3}). Experimental temperatures and spectra appear to the left of the figure, and the best-fit calculated line shapes and corresponding τ_c values appear to the right. The resonance of Λ[Li(*S*-thpc12)]$^{+}$ appears downfield from that of solvated Li^{+}.

Because of a smaller $\Delta H_d^{\ddagger}$ and a substantially negative $\Delta S_d^{\ddagger}$, k_d for Λ[Li(*S*-thpc12)]$^{+}$ is much greater than that for Λ[Na(*S*-thpc12)]$^{+}$. Values of $\Delta H_d^{\ddagger}$ and $\Delta S_d^{\ddagger}$ intermediate between those for its lighter analogues cause k_d for Λ[K(*S*-thpc12)]$^{+}$ to be the largest for the three Λ[M(*S*-thpc12)]$^{+}$. The nonsystematic variation of k_d, $\Delta H_d^{\ddagger}$, and $\Delta S_d^{\ddagger}$ with change in M^{+} probably indicates that changes in both solvation energy and strain in the transition state accompanying the change in size of M^{+} contribute to the differences in the decomplexation rate parameters as M^{+} varies. However, our data do not permit the assignment of a particular step as rate-determining in the sequential decomplexation of octadentate Λ*S*-thpc12 from M^{+}.

The second-order complexation constant, k_c ($=k_dK$), is probably the product of the stability constant (K_o) for the encounter complex, where Λ*S*-thpc12 resides in the second coordination sphere of solvated M^{+}, formed at a rate close to diffusion control, and the first-order rate constant for the subsequent rate-determining complexation step. The variation of k_c with M^{+} is 10-fold smaller than that for k_d, consistent with the decomplexation transition state more closely resembling solvated M^{+} and free Λ*S*-thpc12 than Λ[M(*S*-thpc12)]$^{+}$. (Nonsystematic variations in k_d, $\Delta H_d^{\ddagger}$, $\Delta S_d^{\ddagger}$, and k_c with change in M^{+} are also observed for [M(thec12)]$^{+}$ and [M(tmec12)]$^{+}$, where tmec12 is identical to *S*-thpc12 except that the hydroxy protons and the methyl groups are interchanged.[6,7])

The activation parameters for exchange between the equivalent diastereomeric forms of Λ[M(*S*-thpc12)]$^{+}$ and intermolecular ligand exchange on Λ[M(*S*-thpc12)]$^{+}$ are dissimilar, consistent with the two processes proceeding along different paths overall. Nevertheless, because some bond breaking is necessary for the exchange between the equivalent forms of Λ[M(*S*-thpc12)]$^{+}$ to proceed, it is possible that part of this process is the same as that preceding decomplexation. This appears to be supported by the observation that the lability

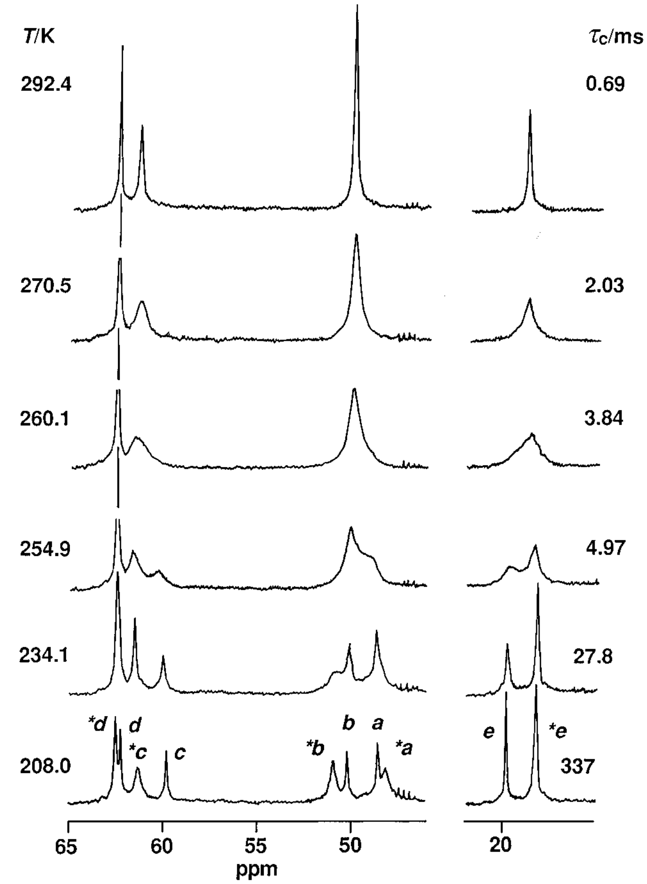

Figure 9. Temperature variation of the broad-band ^{1}H-decoupled 75.47-MHz ^{13}C NMR spectrum of Λ*S*-thpc12 (0.13 mol dm^{-3}) and Λ[Li(*S*-thpc12)]CF_3SO_3 (0.08 mol dm^{-3}), respectively, in methanol-^{12}C-d_4. Experimental temperatures and derived τ_c values appear to the left and the right of the figure, respectively. At 208.0 K, the macrocyclic ring and pendant arm >N*C*H_2−, −*C*H(CH_3)OH, and −CH(*C*H_3)OH carbon resonances of Λ[Li(*S*-thpc12)]$^{+}$ are labeled *a*, *b*, *c*, *d*, and *e*, respectively. The analogous Λ*S*-thpc12 resonances are similarly labeled with the addition of an asterix.

toward the first process follows the M^{+} sequence $K^{+} > Li^{+} > Na^{+}$, which is the same as that for the second.

Λ[M(*S*-thpc12)]$^{+}$ Stability. The stability constant, K = [ΛM(*S*-thpc12)$^{+}$]/([M^{+}][Λ*S*-thpc12]), varies with M^{+} in the sequence $Li^{+} > Na^{+} > K^{+} \approx Rb^{+} \approx Cs^{+}$ in acetonitrile, $Li^{+} > Na^{+} \approx K^{+} > Rb^{+} > Cs^{+}$ in propylene carbonate, $Li^{+} < Na^{+} > K^{+} \approx Rb^{+} \approx Cs^{+}$ in methanol, and $Li^{+} < Na^{+} \approx K^{+} \approx Rb^{+} > Cs^{+}$ in dimethylformamide (Table 3). These variations in stability, and the decrease in K with increase in solvent electron donating power, as reflected by the Gutmann donor number (D_N),[29,30] are consistent with (i) the solvation energy of M^{+}, (ii) the electron donating power of the donor atoms of *S*-thpc12, and (iii) the ability of Λ*S*-thpc12 to assume a conformation that optimizes bonding with M^{+}, dominating the stability of Λ[M(*S*-thpc12)]$^{+}$. Thus, as M^{+} becomes more strongly solvated with an increase in solvent electron donating power (D_N), there is a general decrease in K and the Λ[M(*S*-thpc12)]$^{+}$ stability sequence changes as the balance among i, ii, and iii changes. In methanol, all four pendant arms are coordinated in Λ[M(*S*-thpc12)]$^{+}$ when $M^{+} = Li^{+}$, Na^{+}, K^{+}, and Rb^{+}, and the same is assumed for Cs^{+}. As acetonitrile and propylene carbonate compete less effectively with Λ*S*-thpc12 for M^{+} than does methanol, it is probable that Λ[M(*S*-thpc12)]$^{+}$ is similarly coordinated in these solvents also and

(29) Gutmann, V. *Coordination Chemistry in Nonaqueous Solutions*; Springer-Verlag: Wien, Austria, 1968.
(30) Dewitte, W. J.; Popov, A. I. *J. Soln. Chem.* **1976**, *5*, 231−240.

Table 3. Variation of Λ[M(*S*-thpc12)]$^+$ Stability with M^+ and Solvent at 298.2 K and $I = 0.05$ mol dm^{-3} (NEt_4ClO_4)

		log(K/dm^3 mol^{-1})[a]					
solvent	D_N	Li^+	Na^+	K^+	Rb^+	Cs^+	Ag^+
acetonitrile	14.1[b]	7.65 ± 0.05	5.98 ± 0.05	3.20 ± 0.05	3.16 ± 0.05	3.10 ± 0.05	8.51 ± 0.05
propylene carbonate	15.1[b]	6.7 ± 0.1	5.3 ± 0.1	5.2 ± 0.1	4.8 ± 0.1	4.1 ± 0.1	15.3 ± 0.1
methanol	19.0[b] 23.5[d]	4.0 ± 0.1	4.8 ± 0.1[c]	3.5 ± 0.1	3.4 ± 0.1	3.2 ± 0.1	12.8 ± 0.1
dimethylformamide	26.6[b]	3.24 ± 0.05	3.76 ± 0.05	3.63 ± 0.05	3.56 ± 0.05	3.41 ± 0.05	11.30 ± 0.05
water	18.0[b] 33.0[d]	<2	<2	<2	<2	<2	11.86 ± 0.01

[a] Errors represent one standard deviation. [b] Reference 29. [c] Reference 5. [d] Reference 30.

that coordination changes do not contribute to the variations in stability. The much higher stability of [Ag(*S*-thpc12)]$^+$, by comparison with those of its alkali metal analogues, arises from the strong affinity of soft acid[31,32] Ag^+ for nitrogen donor atoms.[33,34] The decreased stability of [Ag(*S*-thpc12)]$^+$ in nitrogen-donor acetonitrile also arises from this source. In aqueous solution, log(K/dm^3 mol^{-1}) < 2 for the alkali metal Λ[M(*S*-thpc12)]$^+$, while for [Ag(*S*-thpc12)]$^+$, log(K/dm^3 mol^{-1}) = 11.86 ± 0.01 in accord with the above discussion.

The variation of the sequence of the relative magnitudes of K for Λ[M(*S*-thpc12)]$^+$ as the solvent is changed contrasts with the constancy of the sequence of K variation with M^+ for the cryptates. Thus, the cryptates formed by 4,7,13,18-tetraoxa-1,10-diazabicyclo[8.5.5]icosane, [M(C211)]$^+$, exhibit a variation of the magnitude of K with M^+ which is $Li^+ > Na^+ > K^+ > Rb^+ > Cs^+$, and that for the cryptates formed by 4,7,13,16,21-pentaoxa-1,10-diazabicyclo[8.8.5]tricosane, [M(C221)]$^+$, is $Li^+ < Na^+ > K^+ > Rb^+ > Cs^+$ in the solvents considered here.[18] The relatively rigid cavity radii of C211 (80 pm) and C221 (110 pm)[1] more closely approximate the radii of six-coordinate Li^+ (76 pm) and seven-coordinate Na^+ (112 pm)[26] than those of the other M^+ and thereby confer the highest stabilities on [Li(C211)]$^+$ and [Na(C221)]$^+$ while the flexibility of Λ*S*-thpc12 results in lower selectivities and stabilities for Λ[M(*S*-thpc12)]$^+$. Similar K magnitudes and variations with the nature of M^+ and the solvent are seen in the [M(thec12)]$^+$ and [M(tmec12)]$^+$ systems.[6,7]

(31) Pearson, R. G. *J. Am. Chem. Soc.* **1963**, *85*, 3533−3539.
(32) Pearson, R. G. *Coord. Chem. Rev.* **1990**, *100*, 403−425.
(33) Cotton, F. A., Wilkinson, G. *Advanced Inorganic Chemistry*, 5th ed.; Interscience: New York, 1988.
(34) Buschmann, H.-J. *Inorg. Chim. Acta* **1985**, *102*, 95−98.

Conclusion

1,4,7,10-Tetrakis((*S*)-2-hydroxypropyl)-1,4,7,10-tetraazacyclododecane and its alkali metal complex ions exist predominantly as distorted cubic Λ*S*-thpc12 and Λ[M(*S*-thpc12)]$^+$ diastereomers which undergo exchange between equivalent diastereomeric forms in solution. However, a single nitrogen inversion at all four nitrogens of Λ*S*-thpc12 and Λ[M(*S*-thpc12)]$^+$ to produce Δ*S*-thpc12 and Δ[M(*S*-thpc12)]$^+$ (Figure 1) appears to be sterically unfavorable and the latter two diastereomers are undetected. This observation is supported by molecular orbital calculations which yield Λ*S*-thpc12 and Λ[M(*S*-thpc12)]$^+$ as global energy minimized structures. Intermolecular M^+ and Λ*S*-thpc12 exchange on Λ[M(*S*-thpc12)]$^+$ proceeds predominantly through a monomolecular path, and the decomplexation transition state probably resembles solvated M^+ and free Λ*S*-thpc12 more closely than Λ[M(*S*-thpc12)]$^+$. The stabilities of Λ[M(*S*-thpc12)]$^+$ show a variation with both M^+ and the solvent, consistent with the solvation energy of M^+, the electron donating power of the donor atoms of Λ*S*-thpc12, and the ability of Λ*S*-thpc12 to assume a conformation that optimizes bonding with M^+, dominating the stability of Λ[M(*S*-thpc12)]$^+$.

Acknowledgment. Funding of this study by the Australian Research Council and the University of Adelaide and computing resources provided by the South Australian Center for Parallel Computing are gratefully acknowledged.

JA9702071